Nanomembrane-driven co-elution and integration of active chemotherapeutic and anti-inflammatory agents

Erik Pierstorff[1]
Dean Ho[1,2]

[1]Departments of Biomedical
and Mechanical Engineering, Robert
R McCormick School of Engineering
and Applied Science; [2]Robert H
Lurie Comprehensive Cancer
Center, Feinberg School of Medicine,
Northwestern University, Evanston,
IL, USA

Abstract: The release of therapeutic drugs from the surface of implantable devices is instrumental for the reduction of medical costs and toxicity associated with systemic administration. In this study we demonstrate the triblock copolymer-mediated deposition and release of multiple therapeutics from a single thin film at the air-water interface via Langmuir–Blodgett deposition. The dual drug elution of dexamethasone (Dex) and doxorubicin hydrochloride (Dox) from the thin film is measured by response in the RAW 264.7 murine macrophage cell line. The integrated hydrophilic and hydrophobic components of the polymer structure allows for the creation of hybrids of the copolymer and the hydrophobic Dex and the hydrophilic Dox. Confirmation of drug release and functionality was demonstrated via suppression of the interleukin 6 (IL-6) and tumor necrosis factor alpha (TNFα) inflammatory cytokines (Dex), as well as TUNEL staining and DNA fragmentation analysis (Dox). The inherent biocompatibility of the copolymeric material is further demonstrated by the lack of inflammation and apoptosis induction in cells grown on the copolymer films. Thus a layer-by-layer anchored deposition of an anti-inflammatory and chemotherapeutic functionalized copolymer film is able to localize drug dosage to the surface of a medical device, all with an innate material thickness of 4 nm per layer.

Keywords: co-elution, combinatorial therapy, nanomedicine, drug delivery, chemotherapy, inflammation

Introduction

The application of therapeutic drugs to a patient can lead to numerous complications. Most anti-cancer chemotherapies lack cellular specificity, thus systemic administration inevitably causes adverse reactions in patients (Sridhar et al 1992; Gerweck et al 1999; Wang et al 1999; Kimura et al 2000; Kang et al 2002; Olson et al 2003) through the indiscriminate induction of cell death (Arola et al 2000; Kotamraju et al 2000; Wang et al 2004; Eom et al 2005; Hou et al 2005) of cancerous and noncancerous tissues. Likewise, systemically administered anti-inflammatory steroids have been shown to interfere with other treatments. For example, the administration of glucocorticoid anti-inflammatories used to treat inflammatory conditions in cells can interfere with the progression of apoptosis by various anti-cancer chemotherapies, including paclitaxel and doxorubicin (Moran et al 2000; Mikosz et al 2001; Wu et al 2004). The intersection of nanomaterials and medicine has generated platform technologies incorporating various methodologies for film-based drug release and particle based systemic drug administration and circulation. Nanoparticles engineered to contain targeting elements can produce a desired response in cells that present upregulated markers that are indicative of the targeted condition (eg, cancerous, diseased). Nanoparticle based therapeutic delivery systems include diamond-based materials (Chen et al 2007; Huang et al 2007, 2008), metallic nanoparticles (Oishi et al 2006; Rosi et al 2006), and functionalized micelles and

Correspondence: Erik Pierstorff/Dean Ho
2145 Sheridan Road, Evanston, IL
60208, USA
Tel +1 847 467 0548
Fax +1 847 491 3915
Email e-pierstorff@northwestern.edu/
d-ho@northwestern.edu

liposomes (Yoo et al 2001, 2004; Greish et al 2004). Film-based local-release modalities have further been employed for drug therapy which generate a concentrated response at the site of implantation and do not rely on systemic drug transport. These thin film technologies include coatings to protect implants against breakdown/degradation through inflammatory immune responses (Ariga et al 2006; Pierstorff and Ho 2007; Chow et al 2008). Due to the localized and directed nature of this film based therapy, it is a platform through which a wide variety of clinical conditions can be targeted.

Previously, we have demonstrated the use of polymethyloxazoline–polydimethylsiloxane–polymethyloxazoline (PMOXA–PDMS–PMOXA) block copolymer membranes for harnessing and releasing active anti-inflammatory and anti-cancer therapeutics (Chow et al 2008; Pierstorff et al 2008). This copolymer contains both hydrophilic and hydrophilic blocks which allows for the formation of copolymer-drug hybrids that incorporate therapeutics of virtually any type regardless of its hydrophilic or hydrophobic characteristics (Nardin et al 2000, 2001; Ho et al 2003, 2004). The polymer has also been shown to be biocompatible and is only 4 nm thick, making it noninvasive and an ideal candidate for a film based drug eluting platform for medical devices. This study has combined the benefits of thin film polymers with localized drug delivery to fabricate a block copolymer nanofilm capable of eluting multiple therapeutics from a single device (Figure 1). These include dexamethasone (Dex), a steroid based anti-inflammatory and doxorubicin hydrochloride (Dox), an anti-cancer therapeutic that induces cell death via apoptosis. Surface pressure isotherms were used to confirm film formation and drug mixing, and quantitative reverse transcriptase-polymerase chain reaction (RT-PCR), TUNEL-based cell staining, and DNA fragmentation studies were performed to ascertain drug release and function. Thus a multifunctional thin film coating to address multiple conditions simultaneously was created.

Materials and methods
Raw 264.7 murine macrophage culture
RAW 264.7 (ATCC) murine macrophage cells were cultured in $1 \times$ DMEM containing 10% fetal bovine serum (FBS) and
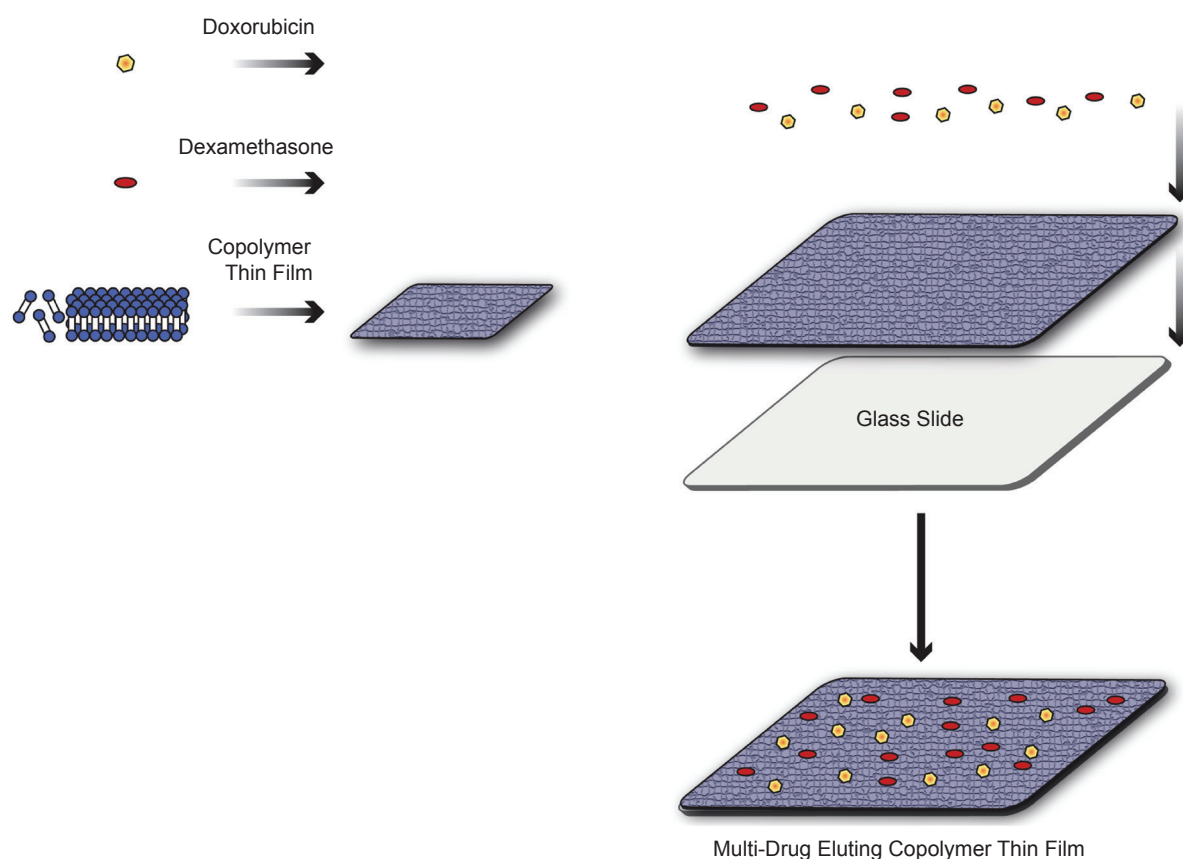

Figure 1 The copolymer-mediated sequestering and integration of multiple therapeutics into a single thin film is shown. Langmuir-Blodgett was used to deposit drug containing triblock copolymer films that can maintain drug incorporation for localized release. Combinatorial therapy at the surface of the material–tissue interface can provide significantly enhanced treatment produced by a noninvasive nanoscale platform. Copyright © 2008. Adapted from Pierstorff E, Krucoff M, Ho D. 2008. Apoptosis induction and attenuation of inflammatory gene expression in murine macrophages via multitherapeutic nanomembranes. *Nanotechnology*, 19:265103–12.

1% penicillin/streptomycin at 37 °C with 5% carbon dioxide. Cells were plated onto the fabricated substrate slides (glass, polymer only, or polymer–drug) and grown for the indicated time points. For inflammation studies, 5 ng/mL lipopolysaccharide (LPS) (Sigma, St. Louis, MO) was added for the last 4 hours of incubation followed by cell harvesting. For apoptosis studies, an additional 10% of FBS was added to the cell culture every 24 hours to prevent serum starvation.

Anti-inflammatory and chemotherapeutic Langmuir–Blodgett film fabrication

Langmuir–Blodgett (LB) films were fabricated using a KSV 2000 Standard Langmuir Trough with a Teflon® base, Delrin barriers, platinum Wilhemy pressure sensor, and a subphase of water. The entire trough was covered with a plastic case with an integrated door to enable manual manipulation/cleaning of the trough. The base was cleaned with multiple washings with methanol and nanopure water using a lint free wipe to ensure trough cleanliness and the trough was then filled with nanopure water. The Wilhemy platinum pressure sensing plate (stored in MeOH) was thoroughly rinsed using nanopure water and heat-sterilized just before use. The pressure sensor was zeroed immediately prior to film deposition or isotherm reading.

Dexamethasone (Sigma) was dissolved in 100% ethanol to a concentration of 5 mg/ml and Doxorubicin (US Pharmacopeia, Rockville, MD) was dissolved in nanopure water to a concentration of 2.5 mg/ml. The drugs (60 µl dexamethasone, 400 µl doxorubicin) were then added to an interfacial pre-formed 20 mN/m copolymer film (Polymer Source, Montreal, QU, Canada) and changes in surface pressure were monitored to confirm drug presence at the air-water interface. After 30 minutes of allowing the film to reach equilibrium, compressions were performed at a rate of 1mm/min to a maximum pressure of 25 mN/m for LB deposition onto glass slides (25 mm × 75 mm) at a rate of 1mm/min. Films were compressed to >50 mN/m until collapse for Langmuir film characterization of film properties. Three layers of drug-functionalized polymer were deposited and used for the studies.

Polymer–dexamethasone-driven suppression of inflammatory gene expression

RAW 264.7 cells were plated onto the fabricated substrate slides (glass, polymer only, or polymer–drug) and grown for 24 hours at 37 °C with 5% carbon dioxide. Cells were stimulated with LPS for 4 hours, followed by cell harvesting. RT-PCR was performed for gene expression

analysis to reflect film functionality as described previously (Pierstorff et al 2008). Briefly, TRIzol reagent (Invitrogen, Carlsbad, CA) was added to each sample to collect the RNA. Subsequent RNA isolation was performed according to the manufacturer's protocol, RNA was converted to cDNA using the I-script enzyme (Bio-Rad, Hercules, CA). Real time PCR analysis (Bio-Rad) was performed monitoring the expression of the genes interleukin 6 (IL-6) and tumor necrosis factor alpha (TNFα) at each time point. Control primers (β-actin) were used to normalize for cDNA concentration variation. Primer sequences utilized are as follows: TNFα: 5'-GGTGCCTATGTCT-CAGCCTCTT-3' and 5'-CGATCACCCCGAAGTTCAGT1, IL-6: 5'-CACAGAGGATAC-CACTCCCAACA-3' and 5' TCCACGATTTCCCAGAGAACA-3', β-actin: 5'-TGGAATCCTGTGGCATCCATGAAAC-3' and 5'-TAAAACGCAGCTCAGTAACAGTCCG-3'.

DNA fragmentation assay for chemotherapeutic nanofilms

RAW 264.7 cells were plated onto the fabricated substrate slides (glass, polymer only, or polymer–drug) and grown for 67 hours at 37 °C with 5% carbon dioxide. Cultures were supplemented with an additional 10% FBS every 24 hours to prevent serum starvation. Cellular DNA was purified as described previously (Huang et al 2007). Briefly, cells were lysed in 500 µL lysis buffer (10 mM Tris-HCl, pH 8.0, 10 mM EDTA, 1% Triton X-100) follwed by 30-minute incubations with RNase A and proteinase K, separately. After phenol chloroform extraction, nuclear DNA was precipitated in isopropyl alcohol, washed in 70% ethanol, and resuspended in DEPC water. Samples were electrophoresed on 0.8% agarose gel, and stained with ethidium bromide.

Confocal microscopy for TUNEL assay

RAW 264.7 cells were plated onto the fabricated substrate slides (glass, polymer only, or polymer–drug) and grown for 67 hours at 37 °C with 5% carbon dioxide. Cultures were supplemented with an additional 10% FBS every 24 hours to prevent serum starvation. The TUNEL based ApopTag® Plus Fluorescein *In Situ* Apoptosis Detection Kit (Chemicon International, Temecula, CA) was used for cell staining to detect apoptosis positive cells following the manufacturer's protocol. Propidium iodide was used for counterstain. Cells were imaged using a Leica inverted microscope Confocal Laser Scanning System and a 40x oil immersion objective. Images were obtained using the Leica Confocal imaging software. Fluorescein was excited at a wavelength of 494 nm

and emission was monitored at 518 nm. Propidium iodide was excited at a wavelength of 536 nm and emission was monitored at 617 nm.

Results

Anti-inflammatory-chemotherapy copolymeric nanofilm fabrication

Mixtures of copolymers with the drugs Dex and Dox were characterized via Langmuir isotherms and copolymer–Dex–Dox thin films were fabricated via Langmuir–Blodgett deposition. Figure 2 shows the compression isotherms for the PMOXA–PDMS–PMOXA triblock copolymer nanofilm alone or mixed with Dox, Dex, or both Dex and Dox. The variations in the isotherms of the copolymer–drug mixtures demonstrate that the readings were responsive to varied drug amounts and that this mixture was able to generate high surface pressure readings indicative of film formation. These graphs show that drug integration into the copolymer film occurs due to changes between compression phase transitions and maximum collapse pressures. These graphs are similar to the variations in surface pressure that have been seen when drugs have been incorporated into a copolymer thin film at the air-water interface using Langmuir–Blodgett (Pierstorff et al 2008). Copolymer films mixed with either Dex or Dox alone have been previously characterized and demonstrate incorporation of either drug into the copolymer matrix (Chow et al 2008; Pierstorff et al 2008). Interestingly, when both Dox and

Dex are mixed with the copolymer nanofilm and compressed, the isotherm completely overlaps that of copolymer and Dex alone. Thus, even though the copolymer–Dox mixture alone has a shift in the isotherm (Figure 2; Pierstorff et al 2008), it appears that this is masked or overwhelmed by the presence of Dex in the mixture as well. While the mechanism driving this observation was unclear, Dox activity assays revealed its incorporation into the copolymer nanofilm.

Polymer–dexamethasone-induced suppression of inflammatory gene expression

Dex incorporation and release from the deposited polymer–Dex–Dox thin films was monitored via the inflammation of cells grown on the polymer–Dex–Dox films with LPS followed by quantitative RT-PCR trials to examine the Dex-mediated suppression of IL-6 and TNFα expression (Figures 3A and 3B). IL-6 gene expression was significantly lower in cells grown on polymer–Dex–Dox films, suggesting that the drug was both present in the film and accessible to the cells frown on the slide (Figure 3A). As a control for Dex mediated cellular inflammation suppression, aqueous Dex was added directly to the media of cells inflamed with LPS. The reduction in IL-6 expression was comparable in cells grown on the polymer–Dex–Dox films (Figure 3A). Furthermore, the TNFα locus was used as an additional demonstration of inflammation reduction in cells grown on
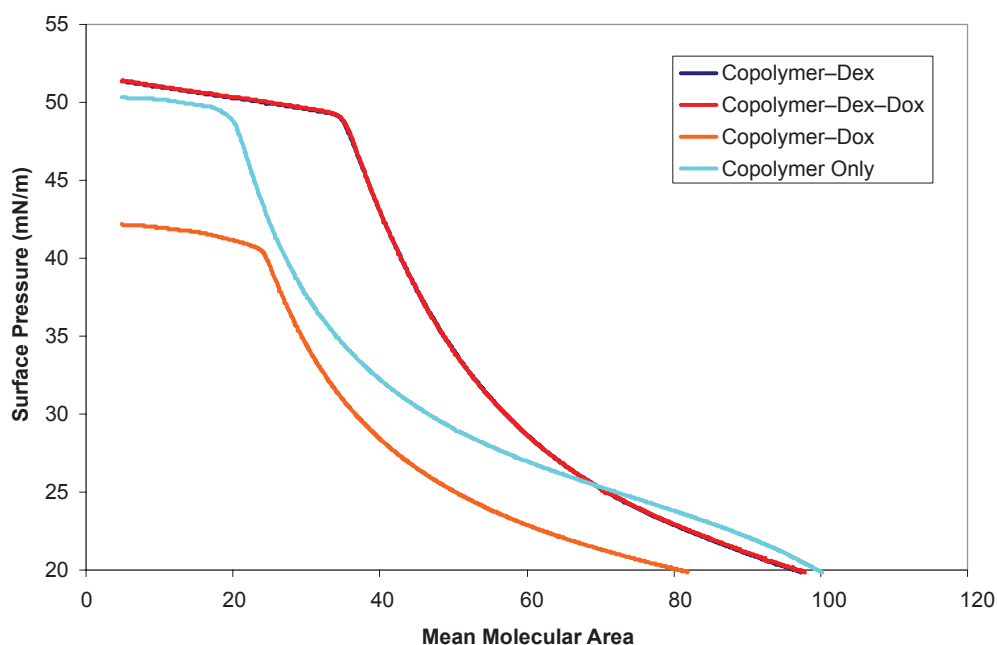

Figure 2 Confirmation of doxorubicin hydrochloride and dexamethasone drug incorporation into the PMOXA–PDMS–PMOXA triblock copolymer was performed via monitoring of surface pressure changes of fabricated Langmuir films. Subsequent drug activity trials confirmed the functionality of deposited hybrid material.
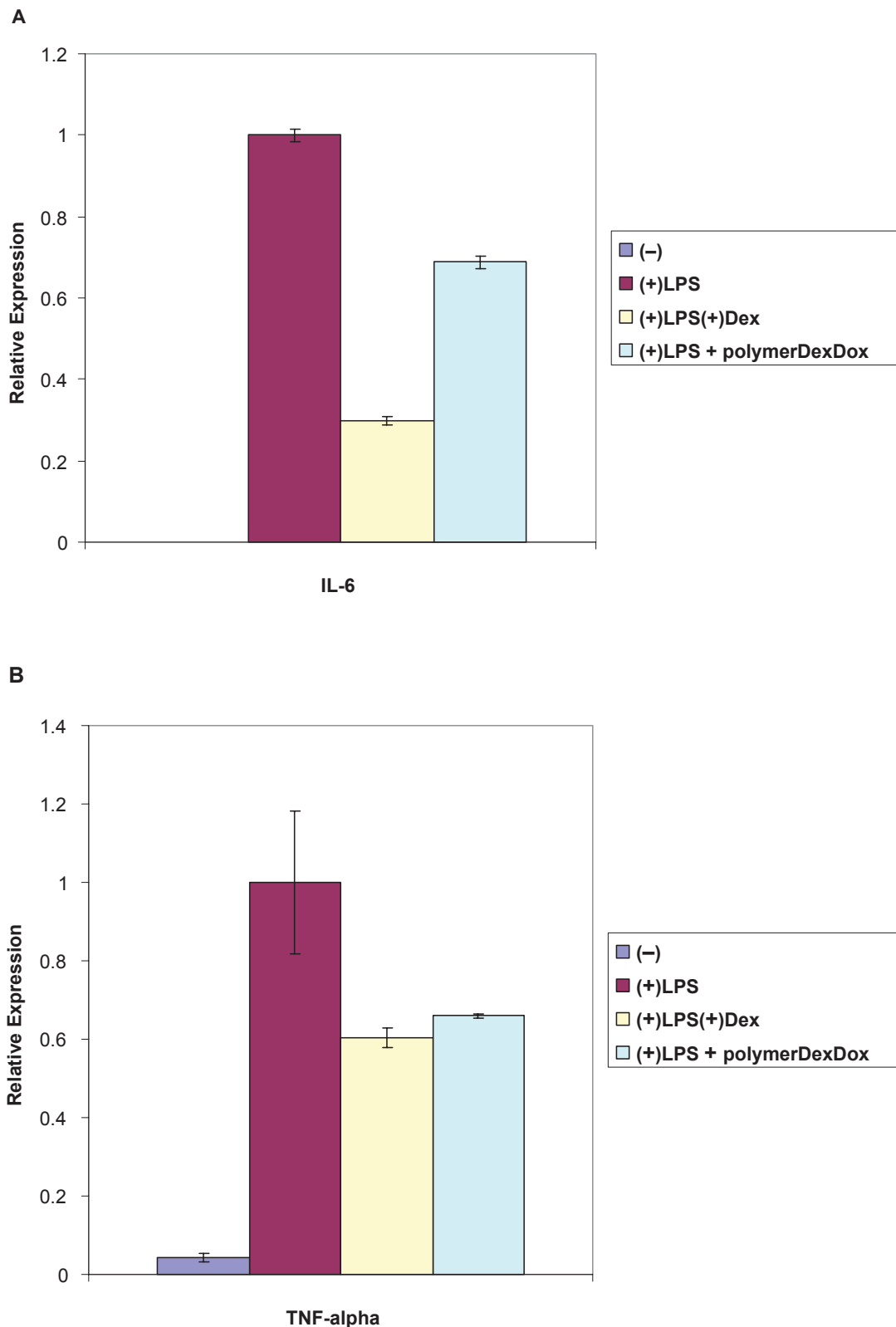
A

IL-6

B

TNF-alpha

Figure 3 A) RT-PCR analysis of IL-6 gene expression was done following macrophage incubation with the polymer–Dex–Dox nanofilms. Gene expression assays with aqueous Dex added were conducted as a control for Dex activity. Results indicated the incorporation of Dex into the copolymer–Dex–Dox thin film and a potent drug releasing activity as shown through a substantial reduction in inflammatory gene expression. **B**) In addition, RT-PCR analysis of TNFα gene expression was done following macrophage incubation with the polymer–Dex–Dox nanofilms. Gene expression assays with aqueous Dex added were conducted as a control for Dex activity. Results further indicated the incorporation of Dex into the copolymer–Dex–Dox thin film and a potent drug releasing activity as shown through a substantial reduction in inflammatory gene expression. The broad suppression of inflammatory gene expression demonstrates an efficient hybrid nanofilm system for an active drug delivery interface. Data was acquired and responses were observed from a minimum of three trials.

polymer–Dex–Dox. As with IL-6, there was significant and comparable reduction of TNFα expression in cells grown on the polymer–Dex–Dox films (Figure 3B).

Doxorubicin-copolymer driven cellular apoptosis

Confirmation of copolymer-mediated Dox incorporation and release from polymer–Dex–Dox was also performed using RAW 264.7 macrophage cells. Studies examining Dox-induced DNA fragmentation as well as apoptosis induction and cellular viability via confocal microscopy

(TUNEL assays) were used to monitor the onset of apoptosis. DNA fragmentation is an indication of cellular apoptosis (Hassan et al 2005). Analysis of polymer–Dex–Dox induced apoptosis was performed via the electrophoresis of cellular DNA and looking for the accumulation of the characteristic laddering of fragmented DNA. The polymer–Dex–Dox hybrids generated a very pronounced DNA fragmentation pattern comparable to that of polymer–Dox hybrids previously characterized, thus demonstrating that Dox was both present in the copolymer films and accessible to the cells grown on the films (Figure 4). Both the glass-only and the
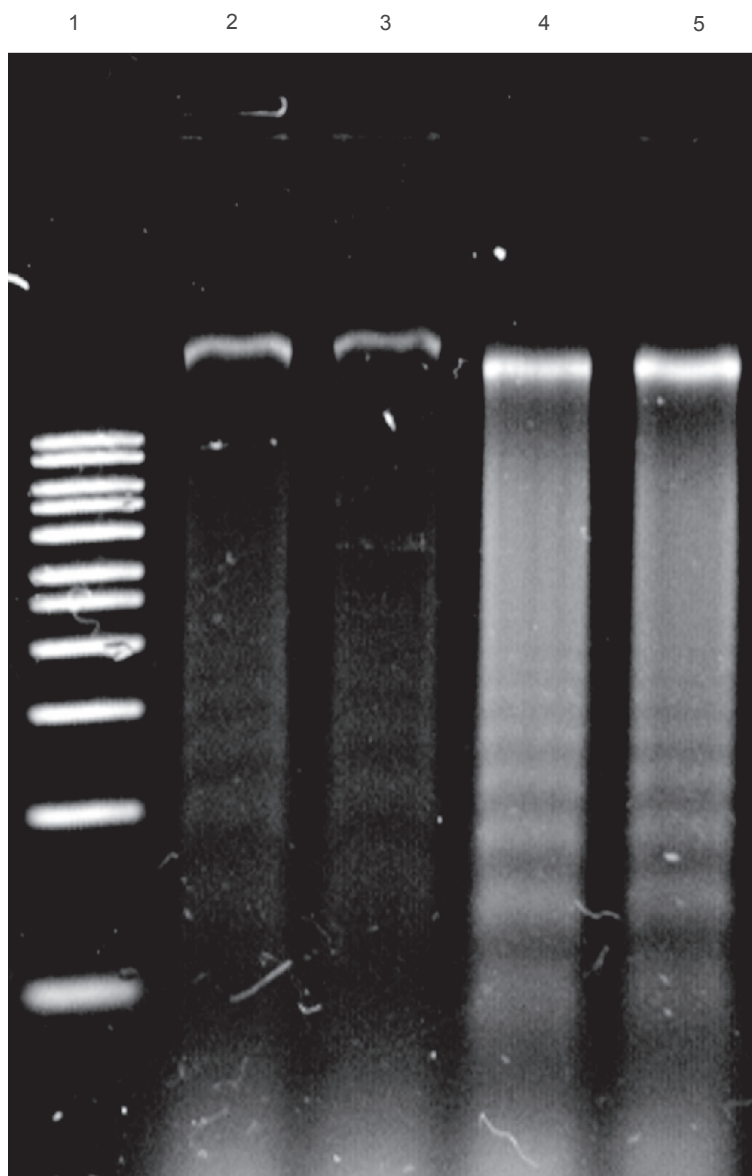

Figure 4 DNA fragmentation assays revealed the preserved functionality of Dox in polymer–Dex–Dox nanofilms. Lane 1 is a DNA marker. Lane 2 represents the control without polymer or drug. Lane 3 represents the culturing of macrophages atop polymer only substrates. Lane 4 represents the polymer–Dox hybrid activity as shown through the clear fragmentation of DNA. Lane 5 represents the polymer–Dex–Dox hybrid activity as shown through the clear fragmentation of DNA. Controlled and localized chemotherapeutic release would significantly enhance the efficacy of cancer treatment via the reduction of systemic toxicity due to systemic administration. The lack of DNA fragmentation or cell death of cells grown on the copolymer substrate highlight the biocompatible properties of the copolymer.

polymer-only control conditions revealed the absence of DNA laddering, thus demonstrating the induction of apoptosis from the polymer–Dex–Dox hybrids as Dox-dependent and providing further supporting evidence for the biocompatibility of the copolymer nanofilm.

Confocal microscopy also revealed the impact of Dox elution from the copolymeric nanofilm upon cellular morphology and apoptosis progression via a TUNEL based staining assay (Figure 5). The polymer–Dex–Dox and polymer–Dox hybrids produced enlarged cellular morphologies that were indicative of pre-apoptotic cells. Glass-only and polymer-only control slides produced cells with unaltered morphologies. In addition, though the same number of cells were seeded per slide, significantly fewer cells grew and propagated on the polymer–Dex–Dox and polymer–Dox hybrid slides. When staining for double stranded breaks indicative of apoptosis progression, none was seen in cells grown on glass or polymer only slides. However, in both the polymer–Dox and the polymer–Dex–Dox slides, an accumulation of apoptotic cells is observed (Figure 5). This is detected both
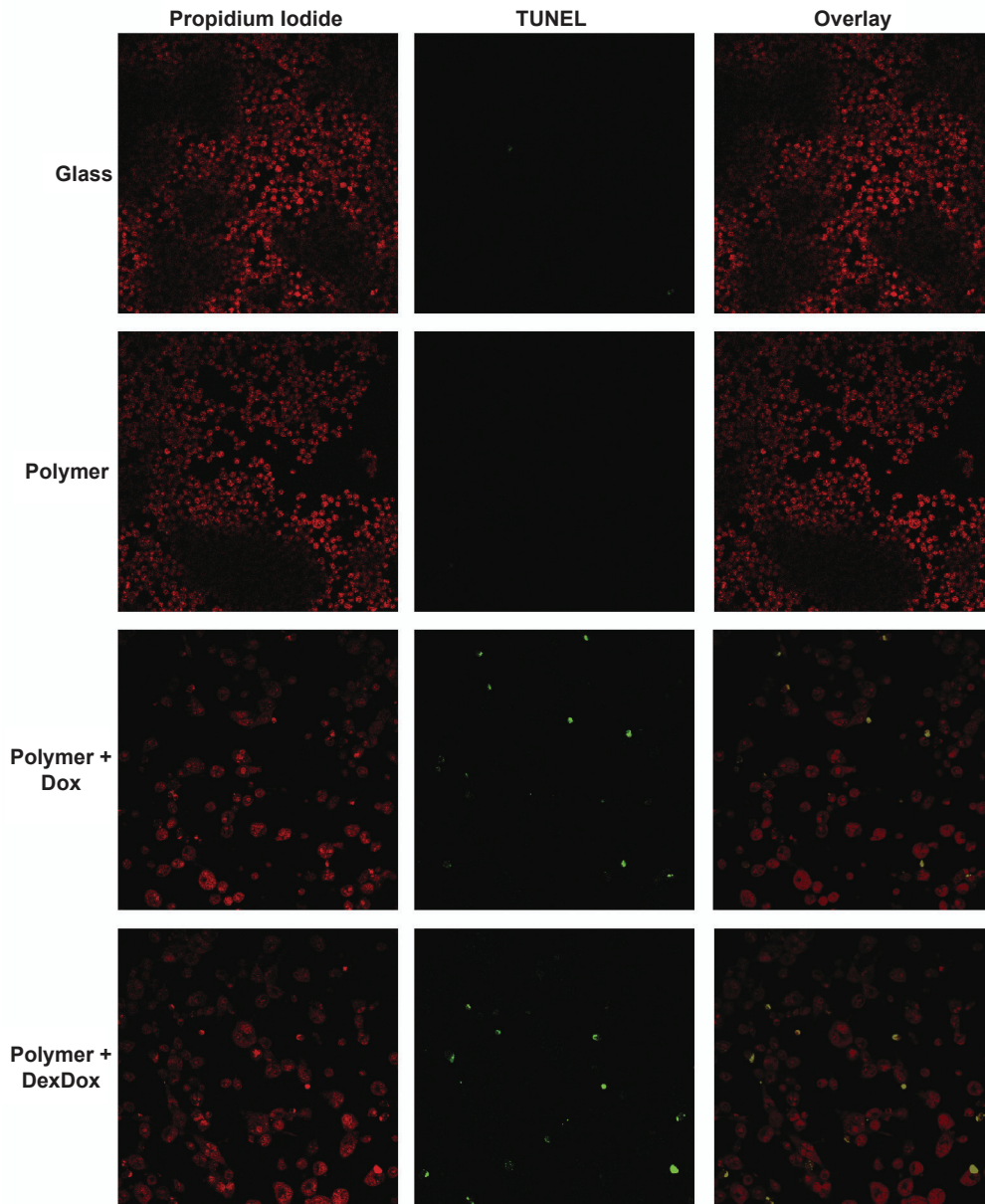

Figure 5 Microscopy Dox impact upon cellular proliferation and morphology was demonstrated via confocal microscopy. Macrophages cultured atop glass or polymer only substrates produced highly confluent growth. Macrophages cultured atop polymer–Dox and polymer–Dex–Dox nanofilm hybrids generated decrease cell confluency, enlarged, preapoptotic cells, as well as shrunken apoptotic cells due to Dox-induced cell death/apoptosis. TUNEL assays demonstrate the progression of cells grown on polymer–Dox and polymer–Dex–Dox nanofilm hybrids to apoptosis.
Notes: Magnification: 40X, Leica inverted microscope Confocal Laser Scanning System.

by the TUNEL stain accumulation and also the shrinking of the apoptotic cells from their pre-apoptotic morphology. Once again this demonstrates a potent Dox dependent apoptosis inducing functionality to the polymer–Dex–Dox films.

Discussion and conclusions

As was previously described, PMOXA-PDMS-PMOXA block polymer based hybrid films can act as platforms for localized drug elution (eg, from an implant surface) and be used as an alternative to systemic drug release (Chow et al 2008; Pierstorff et al 2008). As such, equivalent, or even greater, drug administration at the desired site can be achieved using this technology than from widespread drug delivery, thus increasing efficacy of treatment. In this study, a dual-therapeutic eluting polymer-hybrid film was constructed that releases functional anti-inflammatory (Dex) and anti-cancer drugs (Dox). This suggests that the triblock copolymer can provide the both therapeutics to a location from a single device and could be a more effective drug delivery strategy than systemic/solution-based elution. The Langmuir-Blodgett methodology is an excellent proof of concept for the co-deposition of multiple drugs and copolymer at the air–water interface. Continued work will investigate higher throughput deposition methods.

It is vital to incorporate anti-inflammatory functionality to any drug eluting implantable medical device. The decrease in inflammation will counteract the foreign body response and increase the lifespan of the implanted device and, in the case of an anti-cancer therapeutic drug eluting coating, prolong the time of effective drug release from the device. In addition, increases in IL-6 expression can counteract or have negative impacts on chemotherapy. For example, chronic inflammation can cause apoptosis in various tissues and even induce the onset of cancer (Hjelstrom 2001; Palapattu et al 2005), thus, not only increasing the danger of implantation, but also negating the anti-cancer properties of a chemotherapy eluting device. IL-6 has also been implicated in prostate cancer progression via multiple signaling pathways (Giri et al 2001; Park et al 2003), tumor angiogenesis and inflammation (Hirano et al 1997; Taga and Kishimoto 1997; Giri et al 2001; Willenberg et al 2002), tumor progression and pathogenesis (Siegall et al 1990). As such, both the absence of inflammation from cellular–nanopolymer interaction and the incorporation of anti-inflammatory drugs from its matrix make the polymer-hybrid films extremely promising towards clinical and applied nanomedicine.

Acknowledgments

References

Ariga K, Nakanishi T, Michinobu T. 2006. Immobilization of biomaterials to nano-assembled films (self-assembled monolayers, Langmuir-Blodgett films, and layer-by-layer assemblies) and their related functions. *J Nanosci Nanotechnol*, 6:2278–301.

Arola OJ, Saraste A, Pulkki K, et al. 2000. Acute doxorubicin cardiotoxicity involves cardiomyocyte apoptosis. *Cancer Res*, 60:1789–92.

Chen M, Huang B, Shin E, et al. 2007. Engineering multifunctional biologically-amenable nanomaterials for interfacial therapeutic delivery and substrate-based cellular interrogation. *IEEE Proc BIBE*, 7:517–23.

Chow EK, Pierstorff E, Cheng G, et al. 2008. Copolymeric nanofilm platform for controlled and localized therapeutic delivery. *ACS Nano*, 2:33–40.

Eom YW, Kim MA, Park SS, et al. 2005. Two distinct modes of cell death induced by doxorubicin: apoptosis and cell death through mitotic catastrophe accompanied by senescence-like phenotype. *Oncogene*, 24:4765–77.

Gerweck LE, Kozin SV, Stocks SJ. 1999. The pH partition theory predicts the accumulation and toxicity of doxorubicin in normal and low-pH-adapted cells. *Br J Cancer*, 79: 838–42.

Giri D, Ozen M, Ittmann M. 2001. Interleukin-6 is an autocrine growth factor in human prostate cancer. *Am J Pathol*, 159:2159–65.

Greish K, Sawa T, Fang J, et al. 2004. SMA–doxorubicin, a new polymeric micellar drug for effective targeting to solid tumours. *J Control Release*, 97:219–30.

Hassan F, Islam S, Mu MM, et al. 2005. Lipopolysaccharide prevents doxorubicin-induced apoptosis in RAW 264.7 macrophage cells by inhibiting p53 activation. *Mol Cancer Res*, 3:373–9.

Hirano T, Nakajima K, Hibi M. 1997. Roles of STAT3 in mediating the cell growth, differentiation and survival signals relayed through the IL-6 family of cytokine receptors. *Cytokine Growth Factor Rev*, 8:241–52.

Hjelmstrom P. 2001. Lymphoid neogenesis: *de novo* formation of lymphoid tissue in chronic inflammation through expression of homing chemokines. *J Leukocyte Biol*, 69:331–9.

Ho D, Chu B, Schmidt J, et al. 2003. Hybrid protein/polymer biomimetic membranes. *IEEE Proc Nanotechnol*, 3:379–82.

Ho D, Chu B, Lee H, et al. 2004. Protein-driven energy transduction across polymeric biomembranes. *Nanotechnology*, 15:1084–94.

Hou M, Chrysis D, Nurmio M, et al. 2005. Doxorubicin induces apoptosis in germ line stem cells in the immature rat testis and amifostine cannot protect against this cytotoxicity. *Cancer Res*, 65:9999–10005.

Huang H, Pierstorff E, Osawa E, et al. 2007. Active nanodiamond hydrogels for chemotherapeutic delivery. *Nano Lett*, 7:3305–14.

Huang H, Pierstorff E, Osawa E, et al. 2008. Protein-mediated assembly of nanodiamond hydrogels into a biocompatible and biofunctional multilayer nanofilm. *ACS Nano*, 2:203–12.

Kang YJ, Sun X, Chen Y, et al. 2002. Inhibition of doxorubicin chronic toxicity in catalase-overexpressing transgenic mouse hearts. *Chem Res Toxicol*, 15:1–6.

Kimura T, Fujita I, Itoh N, et al. 2000. Metallothionein acts as a cytoprotectant against doxorubicin toxicity. *Pharm Exp Ther*, 292:299–302.

Kotamraju S, Konorev EA, Joseph J, et al. 2000. Doxorubicin-induced apoptosis in endothelial cells and cardiomyocytes is ameliorated by nitrone spin traps and ebselen. Role of reactive oxygen and nitrogen species. *J Biol Chem*, 275:33585–92.

Mikosz CA, Brickley DR, Sharkey MS, et al. 2001. Glucocorticoid receptor-mediated protection from apoptosis is associated with induction of the serine/threonine survival kinase gene, sgk-1. *J Biol Chem*, 276:16649–54.

Moran TJ, Gray S, Mikosz CA, et al. 2000. The glucocorticoid receptor mediates a survival signal in human mammary epithelial cells. *Cancer Res*, 60:867–72.

Nardin C, Winterhalter M, Meier W. 2000. Giant free-standing ABA triblock copolymer membranes. *Langmuir*, 16:7708–12.

Nardin C, Widmer J, Winterhalter M, et al. 2001. Amphiphilic block copolymer nanocontainers as bioreactors. *Eur Phys J*, E4:403–10.

Oishi M, Nakaogami J, Ishii T, et al. 2006. Smart PEGylated gold nanoparticles for the cytoplasmic delivery of siRNA to induce enhanced gene silencing. *Chem Lett*, 35:1046–7.

Olson LE, Bedja D, Alvey SJ, et al. 2003. Protection from doxorubicin-induced cardiac toxicity in mice with a null allele of carbonyl reductase 1. *Cancer Res*, 63:6602–6.

Palapattu GS, Sutcliffe S, Bastian PJ, et al. 2005. Prostate carcinogenesis and inflammation: emerging insights. *Carcinogenesis*, 26:1170–81.

Park JI, Lee MG, Cho K, et al. 2003. Transforming growth factor-β1 activates interleukin-6 expression in prostate cancer cells through the synergistic collaboration of the Smad2, p38-NF-κB, JNK, and Ras signaling pathways. *Oncogene*, 22:4314–32.

Pierstorff E, Ho D, 2007. Monitoring, diagnostic, and therapeutic technologies for advanced medicine at the intersection of life science and engineering. *J Nanosci Nanotech*, 7:2949–68.

Pierstorff E, Krucoff M, Ho D. 2008. Apoptosis induction and attenuation of inflammatory gene expression in murine macrophages via multitherapeutic nanomembranes. *Nanotechnology*, 19:265103–12.

Rosi NL, Giljohann DA, Thaxton CS, et al. 2006. Oligonucleotide-modified gold nanoparticles for intracellular gene regulation. *Science*, 312:1027–30.

Siegall CB, Schwab G, Nordan RP, et al. 1990. Expression of the interleukin 6 receptor and interleukin 6 in prostate carcinoma cells. *Cancer Res*, 50:7786–8.

Sridhar R, Dwivedi C, Anderson J, et al. 1992. Effects of verapamil on the acute toxicity of doxorubicin in vivo. *J Natl Cancer Inst*, 84:1653–60.

Taga T, Kishimoto T. 1997. gp130 and the interleukin-6 family of cytokines. *Ann Rev Immunol*, 15:797–819.

Wang GW, Kang YJ. 1999. Inhibition of doxorubicin toxicity in cultured neonatal mouse cardiomyocytes with elevated metallothionein levels. *Pharm Exp Ther*, 288:938–44.

Wang S, Konorev EA, Kotamraju S, et al. 2004. Doxorubicin induces apoptosis in normal and tumor cells via distinctly different mechanisms. *J Biol Chem*, 279:25535–43.

Willenberg HS, Päth G, Vögeli TA, et al. 2002. Role of interleukin-6 in stress response in normal and tumorous adrenal cells and during chronic inflammation. *Ann N Y Acad Sci*, 966:304–14.

Wu W, Chaudhuri S, Brickley DR, et al. 2004. Microarray analysis reveals glucocorticoid-regulated survival genes that are associated with inhibition of apoptosis in breast epithelial cells. *Cancer Res*, 64:1757–64.

Yoo HS, Park TG. 2001. Biodegradable polymeric micelles composed of doxorubicin conjugated PLGA-PEG block copolymer. *J Control Release*, 70:63–70.

Yoo HS, Park TG. 2004. Folate receptor targeted biodegradable polymeric doxorubicin micelles. *J Control Release*, 96:273–83.